

Comparison between Readout-Segmented (RS)-EPI and an improved distortion correction method for Short-Axis Propeller (SAP)-EPI

S. Skare¹, S. J. Holdsworth¹, K. Yeom¹, P. D. Barnes¹, and R. Bammer¹
¹Radiology, Stanford University, Palo Alto, CA, United States

Introduction: ‘Short-Axis readout Propeller EPI’ (SAP-EPI) (1) and ‘Readout-Segmented EPI’ (RS-EPI) (2) have been proposed for use in high resolution diffusion-weighted (DW) imaging (Fig. 1). SAP-EPI and RS-EPI share common characteristics, in that k -space is traversed by several EPI ‘segments’ (referred to as blades (SAP-EPI) or blinds (RS-EPI)) in order to reduce the distortion and blurring that typically hampers EPI images. Previous work comparing RS-EPI and SAP-EPI (3) concluded that SAP-EPI suffers from considerably more blurring compared with RS-EPI despite attempts to correct for distortion. With an improved distortion correction method, we demonstrate that SAP-EPI results in a similar image resolution to RS-EPI for a given SNR normalized for scan time/slice.

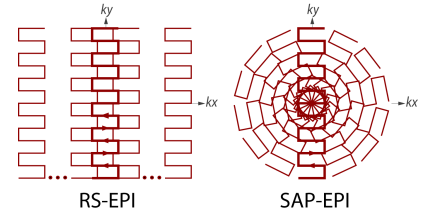


Fig 1: k -space trajectories for RS-EPI and SAP-EPI. RS-EPI requires an extra navigator echo for the DW image resulting in reduced scan efficiency, thus SNR, despite that fewer segments are required to fill k -space. The overlapping blades in the center of k -space in SAP-EPI may also contribute to a higher $\eta = SNR / \sqrt{\text{scan time/slice}}$.

Methods: All images were acquired on a 3T whole-body MRI unit (GE Discovery MR750) using an 8-channel head coil and a high-performance gradient system (50 mT/m, SLR=200 mT/m/s). Scan-time matched SAP-EPI and RS-EPI experiments were first performed on healthy volunteers using two matrix sizes: 256×252 (blade/blind width = 64) and 384×384 (blade/blind width = 96). Other parameters were: FOV = 26 cm, #blades/#blinds = 7, $\Delta z = 5$ mm, TR/TE = 4 s/76 ms, GRAPPA $R = 3$, NEX = 3, partial Fourier with 24 overscans, twice-refocused diffusion preparation, and $b = 1000$ s/mm². The maximum number of slices for SAP-EPI and RS-EPI was 35/31, respectively (matrix size = 252^2) and 35/31 (matrix size = 384^2). Together with noise maps generated from repeated $b = 0$ scans, the scan time efficiency ($\eta = SNR / \sqrt{\text{scan time/slice}}$) was calculated from the RS-EPI and distortion-corrected SAP-EPI images. Patient RS-EPI and SAP-EPI DTI data were then collected on three pediatric patients using a matrix size of 192^2 (blade/blind width = 64, #blades/#blinds = 7, FOV = 20 cm, $\Delta z = 5$ mm, TR/TE = 3000/76 ms, $R = 3$, NEX = 3, partial Fourier (24 overscans), twice refocusing, 1 $b = 0$, 7 isotropic diffusion directions with $b = 1000$ s/mm², scan time = 7:36min). Here, the maximum number of slices that could be selected for SAP-EPI was 25, compared with 19 for RS-EPI. In our previous distortion correction implementation for SAP-EPI (4), the distorted blade data underwent two unnecessary sampling steps which now have been removed. Each of these resampling steps caused a slight loss in resolution, which also added a blur in the final image. For the new implementation presented in this work, we estimate (again only using the blade data itself) the ΔB_0 field in the laboratory space while using the original blade data in their own native coordinate systems, each having their unique 4×4 voxel-to-world matrix (defining its position and rotation) applied to the resampling coordinates.

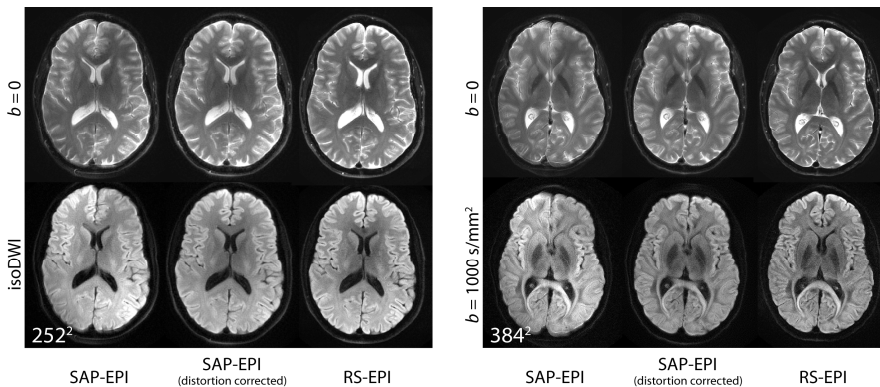


Fig 2: Comparison between SAP-EPI, distortion-corrected SAP-EPI, and RS-EPI on a healthy volunteer at matrix sizes of 252×252 (left) and 384×384 (right). SAP-EPI and RS-EPI datasets were acquired in equivalent scan times of 1:24min/volume.

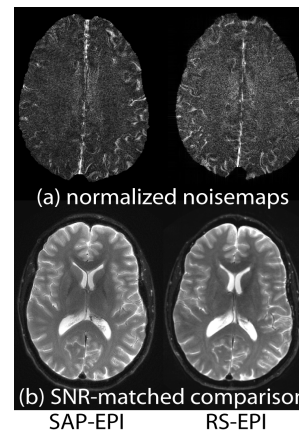


Fig 3: (a) Scan-time-normalized noise maps (i.e. accounting for the maximum number of slices) of distortion-corrected-SAP-EPI and RS-EPI calculated over six $b = 0$ scans (matrix size= 384^2). (b) A RS-EPI 384^2 image is blurred by a Gaussian kernel to achieve the same SNR as SAP-EPI, resulting in a loss of resolution. This shows that distortion-corrected SAP-EPI has better scan efficiency than RS-EPI even at high resolutions.

Results: Fig. 2 shows SAP-EPI, distortion-corrected SAP-EPI, and RS-EPI $b = 0$ and DW images acquired with matrix sizes of 252^2 and 384^2 . The SAP-EPI images show considerably less blurring when corrected for distortion, with a resolution approaching that of the RS-EPI scan. The normalized SNR ratio ($SNR_{SAP-EPI} / SNR_{RS-EPI}$) was 1.3 and 1.6 for the 252^2 and 384^2 matrix sizes, respectively – indicating that one must scan RS-EPI approximately twice as long in order to achieve the same SNR as SAP-EPI. Fig. 3a depicts the normalized noise maps for the 384^2 acquisitions. To correct for the difference in normalized SNR, the RS-EPI images were blurred to achieve the same SNR as SAP-EPI (Fig. 3b), demonstrating that at a comparative SNR the resolution is now very slightly reduced for RS-EPI. Fig. 4 shows pediatric patient data comparing distortion-corrected-SAP-EPI and RS-EPI. SAP-EPI had a higher SNR (particularly evident in the color FA maps) than RS-EPI. Note that RS-EPI appears sharper in the frontal region in the left panel due to incomplete distortion correction at the FOV boundaries.

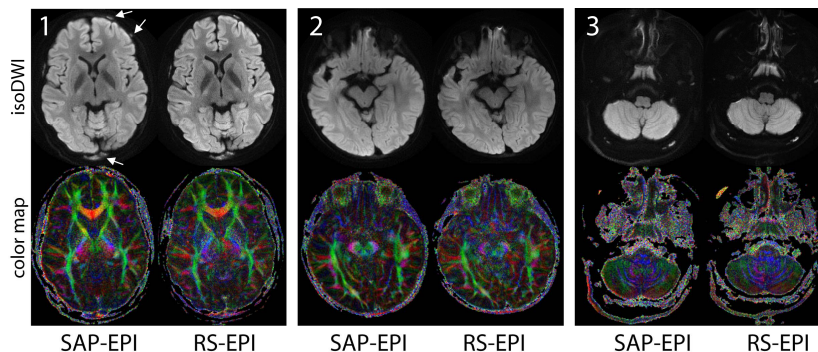


Fig 4: Comparison between distortion-corrected-SAP-EPI and RS-EPI acquired on three pediatric patients (labeled 1 through 3). Both the isoDWI and 1st eigenvector color maps are shown at 3 levels of the brain. Note that patient #1 presented with Ewing’s sarcoma (metastatic spread to the calvarium, white arrows).

Discussion & Conclusion: This study demonstrates that SAP-EPI combined with an improved distortion-correction method and RS-EPI produce images of similar quality. At first glance, distortion-corrected SAP-EPI images (Figs. 2 and 4) appear more blurred than RS-EPI images. Without scan time restrictions, the unidirectional distortions in RS-EPI result in a sharper image, particularly with increasing resolution. However, one must scan RS-EPI approximately twice as long to achieve the same SNR. For an SNR-matched scenario, as shown in Fig. 3, the image quality of the two acquisitions very closely resemble each other – with a slight reduction in resolution for RS-EPI. In addition to the larger slice coverage/TR, SAP-EPI has one important advantage over RS-EPI in that for each blade, the stack of 2D slices forms a ‘brick’ in the image domain, making image domain 3D motion correction possible.

References: [1] Skare S. MRM 2006, 55:1298-1307. [2] Porter D. ISMRM 2008, p3262. [3] Holdsworth S. ISMRM 2008, p1808. [4] Skare S. ISMRM 2008, p417.

Acknowledgements: This work was supported in part by the NIH (1R01EB008706, 1R01EB008706S1, 5R01EB002711, 1R01EB006526, 1R21EB006860), the Center of Advanced MR Technology at Stanford (P41RR09784), Lucas Foundation, Oak Foundation, and the Swedish Research Council (K2007-53P-20322-01-4). Special thanks to Serman Lim, Alfred Barikdar, Allan White, Young Chang, Harold Estrada, Liz Ellison, and Abbie Bird and for their assistance with the patient studies.